Accounts

The Structures and Bonding of Hyperlithiated Molecules

Hiroshi Kudo* **and Keiichi Yokoyama†**

Department of Chemistry, Graduate School of Science, Tohoku University, Sendai 980-77

†Advanced Science Research Center, Japan Atomic Energy Research Institute, Tokai-mura, Ibaraki 319-11

(Received February 2, 1996)

This article describes the nature of bonding in hyperlithiated molecules with stoichiometries exceeding normal valence expectations. The existence of such hyperlithiated or hypervalent molecules as CLi_6, Li_3O, Li_4O, Li_5O, Li_3S, Li_4S, Li_4P, Li_2CN, Na_2CN, and K_2CN has already been experimentally confirmed by means of Knudsen-effusion mass spectrometry in our laboratory. These molecules have nine or more valence electrons, violating, at least formally, the octet rule. However, these molecules are thermodynamically more stable than the corresponding octet molecules. Results of ab initio MO calculations reveal that the extra valence electrons beyond the usual octet are in singly occupied orbitals (SOMO) or highest occupied orbitals (HOMO) in the Li_nA (A = C, O, P, S) molecules. The SOMO as well as HOMO forms the Li–Li bonds between all pairs of lithium atoms and contribute to stabilization of these molecules. The bonding situation of the M_2CN (M = Li, Na, K) species is apparently different from that of Li_nA. The favored structure has C_s symmetry and is best described as a complex of the CN^- anion with the M_2^+ cation. The extra valence electron is in SOMO, which corresponds to the radical cation SOMO and contributions to M–M bonding. The presence of the M_2^+ unit is a typical example of justifying the term hypervalent.

The octet rule[1,2] states that the most stable species is formed in a molecular system of covalent bonds when eight electrons are shared in the valence shell. All of the hydrides of elements in the second- and third-row of the periodic table obey the rule. The typical example is bonding in such hydrides as CH_4, NH_3, and H_2O. However, recent studies have indicated that replacement of the hydrogen atoms by lithium atoms in these hydride molecules changes the feature of the chemical bonds. Experiments by Kudo and Wu[3—12] as well as theoretical work by Schleyer et al.[13,16] have shown the existence of thermodynamically stable polylithiated molecules with nine or more valence electrons; e.g., Li_3O, Li_3S, and Li_4P with nine valence electrons and CLi_6, Li_4O, and Li_4S, with 10 valence electrons. These polylithiated molecules, called hyperlithiated or hypervalent molecules, are thermodynamically more stable than octet molecules with eight valence electrons like Li_2O, Li_2S, and CLi_4. Does the hyperlithiated molecule violate the octet rule?

The hyperlithiated molecules described above exhibit the following characteristics: (1) nine or more electrons bind substituents to the central atom, (2) substituents are comparably distant from the central atom, (3) there is a global energy minimum on the potential energy surface, and (4) molecules are thermodynamically stable toward all possible dissociation products, but not necessarily stable to association or reactions with other molecules. Recently, the existence of another type of hyperlithiated molecule (e.g. Li_2CN) has been confirmed experimentally.[17] The favored structure of Li_2CN obtained by theoretical calculations has C_s symmetry and is best described as a complex of the CN^- anion with the Li_2^+ radical cation.

The study of the nature of bonding in hypervalent molecules is a subject of current interest, and a number of theoretical computations have been conducted on the structure and stability of not only hyperlithiated molecules (CLi_5, CLi_6, Li_4N, Li_5N, Li_3O, Li_4O, Li_2F, Li_3F, Li_3S, Li_4S, Li_4P),[18—27] but also of hypersodium (Na_2O, Na_3O, Na_2Cl),[28—33] hyperpotassium (K_2O, K_3O, K_2Cl),[29,34] hyperaluminum (Al_3O, Al_4O),[35,36] hypermagnesium (Mg_2O, Mg_3O, Mg_4O),[37,38] hypersilicon (Si_2O, Si_3O),[39] and other hypervalent molecules.[40,41] The present paper describes the experimental and theoretical studies on the nature of bonding in hyperlithiated molecules.

The Hyperlithiated Molecules Li_3O and Li_4O

The first hyperlithiated molecule Li_3O was observed in 1978 in the gas phase over Li_2O crystals at elevated temperatures by Kudo and Wu through a mass spectrometric study on vaporization of Li_2O crystals, which were a potential candidate for tritium breeding materials of thermonuclear fusion reactors. The ionization energy observed was 4.5±0.2 eV. The dissociation energy of Li_3O to give Li_2O and Li was

determined as 212±42 kJ mol^{-1}. These experimental results indicated that the Li_3O molecule should be a neutral molecule which had formally nine valence electrons. This molecule is thermodynamically more stable than Li_2O, an octet molecule, because the dissociation reaction

$$Li_3O(g) \longrightarrow Li_2O(g) + Li(g) \quad (1)$$

is endothermic with ΔH_0°=212±42 kJ mol^{-1}. It seems hard to give a reasonable explanation of the formation of the stable Li_3O molecule with nine valence electrons in a context of the octet rule, since the formation of the stable H_3O molecule with nine valence electrons is denied theoretically; the molecular ion H_3O^+ as well as the water molecule (H_2O) with eight valence electrons is thermodynamically stable.

The existence of stable Li_3O was theoretically supported by Schleyer et al. in 1982.[13] They were able to find a global energy minimum on the potential energy surface for Li_3O **1** (Fig. 1) with C_{2v} symmetry by ab initio MO calculations at the 3—21 G level. Later, Schleyer et al. reported that the most stable structure is Li_3O **2** with D_{3h} symmetry.[24] The O–Li bond length (1.682 Å) in Li_3O **2**, a nine valence electron species, is actually shorter than the bond length (1.696 Å) in Li_3O^+ (D_{3h}) **3**, an octet molecule. On the other hand, the stable Li_4O **4** prefers a tetrahedral geometry (T_d). The O–Li bonds are not lengthened significantly. The structures and energies of these hypervalent molecules indicate that the "extra" electrons are neither antibonding nor even nonbonding, but occupy bonding orbitals.

What is the nature of the hyperlvalent bonding in these molecules? Hypervalent molecules with third-row central atoms are common and use low-lying d orbitals. This cannot be the explanation in the second-row, since d orbitals are less readily available energetically; in any case, the phenomenon is found with the 3—21 G basis, which has no d-type functions.[13] Some indication of the nature of bonding can be obtained from the occupied molecular orbitals and the Mulliken analysis. In tetrahedral Li_4O, 10 valence electrons occupy molecular orbitals $(3a_1)^2(2t_2)^6(4a_1)^2$. The $3a_1$ and $2t_2$ orbitals are analogous to the valence orbitals in the tetrahedral CH_4 and CLi_4. Occupation of these four orbitals leads to AX bonding, but not antibonding among the substituent atoms, X. The highest occupied orbital (HOMO) in Li_4O is the totally symmetric orbital $4a_1$ with an additional radial node. However, the $4a_1$ orbital is bonding between all pairs of lithiums. Since the eight electrons in $3a_1$ and $2t_2$ largely fill the octet on the oxygen atom, $4a_1$ has large coefficients on lithium atoms (particularly the diffuse outer function of the 3—21 G Li basis). It follows that the contribution to Li–Li bonding from six pair-wise combinations is quite large.

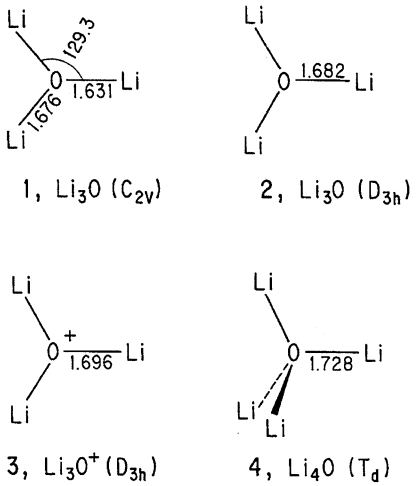

Fig. 1. Optimized structures of Li_3O, Li_3O^+, and Li_4O calculated by Schleyer et al.[13,24] at HF/3-21 G for **1**, **4** and MP2(FU)/6-31+G* for **2**, **3**; the bond distance in Å.

To our astonishment, the further computations by Schleyer's group have predicted the formation of a variety of stable hyperlithiated molecules; e.g. CLi_5, NLi_4, and FLi_2 with nine valence electrons, CLi_6, NLi_5, and FLi_3 with 10 valence electrons, and Li_5O and FLi_4 with 11 valence electrons.[15] Table 1 summarizes the dissociation energies of hyperlithiated or hypervalent molecules, the existence of each of which has eventually been confirmed experimentally.[3—12,42—45]

Hyperlithiated Molecule CLi_6

Of hyperlithiated molecules listed in Table 1, CLi_5 and CLi_6 have attracted great interest of theoretical chemists as well as organic and organometallic chemists. The molecular configurations of CLi_5 (D_{3h}) **5** and CLi_6 (O_h) **6** are highly symmetrical as shown in Fig. 2. These molecules are thermodynamically more stable than CLi_4 with eight valence electrons.[14] Namely, theoretical calculations by Schleyer's group have indicated that the following dissociation reactions

$$CLi_5(g) \longrightarrow CLi_4(g) + Li(g) \quad (2)$$

$$CLi_6(g) \longrightarrow CLi_4(g) + Li_2(g) \quad (3)$$

are endothermic with ΔH_0°=226 and 273 kJ mol^{-1}, respectively.

According to the Schleyer's ab initio MO calculations,[14] the C–Li bond lengths in CLi_5 **5** and CLi_6 **6** are only slightly longer than those found for CH_3Li (2.001 Å) or CLi_4 (1.929 Å) at the 3—21 G basis set, showing that all the lithiums are bound to carbon. In octahedral symmetry, the occupancy of the 10 valence electrons is $(3a_{1g})^2(2t_{1u})^6(4a_{1g})^2$. The $3a_{1g}$ and $2t_{1u}$ orbitals are analogous to the valence orbitals found in T_d or O_h symmetry. If only four valence orbitals are occupied, C–Li bonding results, but the Li–Li contacts are antibonding.

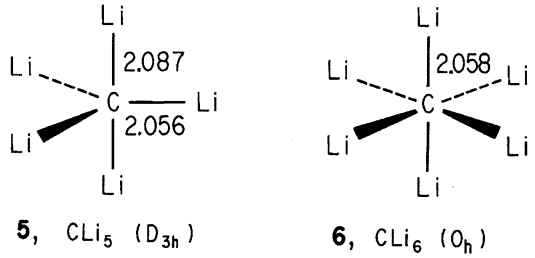

Fig. 2. Optimized structures of CLi_5 and CLi_6 calculated by Schleyer et al.;[13] the bond distance in Å.

Table 1. Dissociation Energies of Hyperlithiated Molecules: $Li_nA \rightarrow Li_{n-1}A+Li$

Number of formal valence electrons	Molecules (Point group)	D_0°/kJ mol^{-1}		
		Theoretical		Experimental
		Schleyer et al.	Kudo et al.	Kudo et al.
9	CLi_5 (D_{3h})	226.4	—	—
	Li_3O (D_{3h})	198.3	—	212±42
	Li_3S (C_{3v})	141.8	148.5	138±14
	Li_4P (T_d)	141.8	—	186±24
10	CLi_6 (O_h)	59.4	—	—
		(273)[a)]	—	(274±11)[a)]
	Li_4O (T_d)	120.9	—	197±30
	Li_4S (C_{2v})	123.2	102.5	212±13
11	Li_5O (C_{3v})	65.7	—	121±25
	Li_2CN (C_s)	—	103.8	137±14
	Na_2CN (C_s)	—	72.8	104±14
	K_2CN (C_s)	—	74.5	82±8

a) $CLi_6(g) \rightarrow CLi_4(g)+Li_2(g)$ process.

However, the HOMO in the 10 valence electron species, CLi_6, is totally symmetric ($4a_{1g}$) and possesses an additional spherical node. The Li–Li bonding character of this $4a_{1g}$ orbital is revealed by the positive overlap populations and the large coefficients on the lithium atoms. The 12 pair-wise bonding contacts between adjacent lithium atoms in CLi_6 contribute significant stabilization to the whole system.

The indicated charges (3—21 G) on carbon do not increase appreciably as more lithium atoms are added: CLi_4 (C, −0.81), CLi_5 (C, −0.81), and CLi_6 (C, −0.93). Thus, the extra electrons in the effectively hypervalent molecules, CLi_5 and CLi_6, are not associated with carbon, which remains content with its normal octet. The extra electrons beyond the usual octet are involved with Li–Li bonding and help to build a metallic "cage" around the central atom. The feature of bonding is depicted in Fig. 3.

To confirm the theoretical prediction, Kudo[5,9,10] conducted experiments with a specially designed Knudsen-effusion mass spectrometer illustrated in Fig. 4. The apparatus consists of a cross-beam ionizer, a quadrupole mass filter, and an electron multiplier with a conversion dynode, all of which are installed in an ultrahigh vacuum (UHV) chamber. The background pressure of the UHV system was kept below 6×10^{-7} Pa at room temperature and 4×10^{-5} Pa during the measurements at elevated temperatures. Lithium carbide (Li_2C_2) crystals were loaded in a molybdenum Knudsen cell and heated by a radiofrequency generator. The cell temperature, controlled with ±5 K at 1000 K, was measured with both a thermocouple (R-type) embedded at the bottom of the cell and an optical pyrometer, which were calibrated in situ at the triple points of Al and Ag. The volume of the Knudsen cell was 1.5 cm^3 and the orifice diameter was 0.3

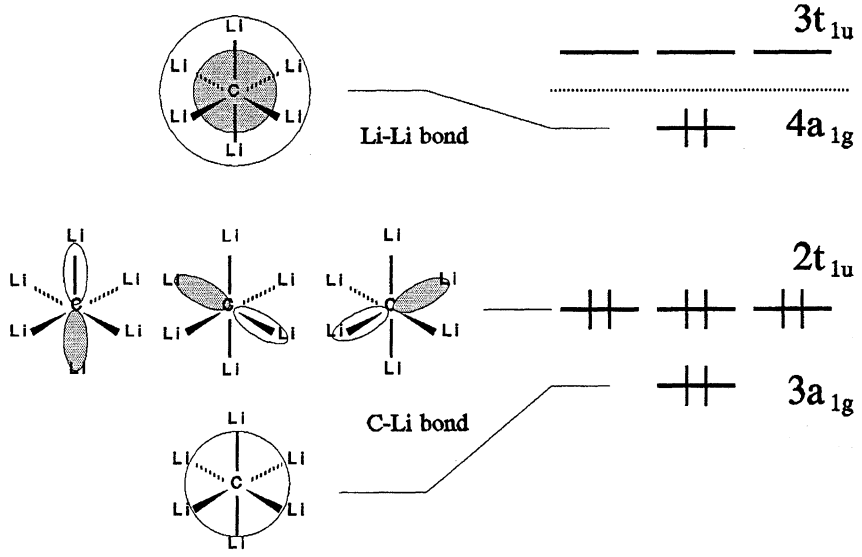

Fig. 3. Features of valence molecular orbitals in CLi_6 molecule. Extra valence electrons are in $4a_{1g}$ orbital (HOMO) that is antibonding between the Li and C, but bonding between all pairs of Li atoms.

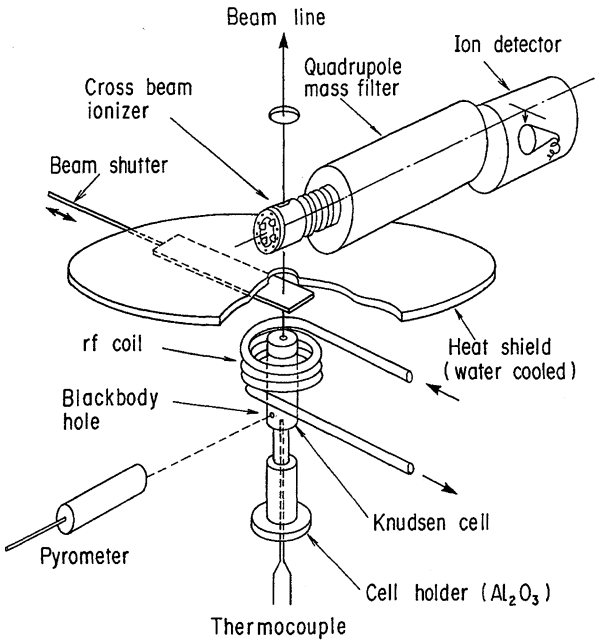

Fig. 4. A sketch of Knudsen-effusion mass spectrometer installed in UHV system.

mm. Molecular species effusing from the cell were directly introduced into the ionizer. A shutter was inserted between the cell and the ionizer to discriminate the molecular beam from the residual gas; molecular species in the beam were analyzed by the mass spectrometer only when the shutter was open.

The effusing gaseous species were ionized by electron impact at the energy around 5 eV higher than the ionization energy of molecules to be detected. Identification of the species was achieved from their mass-to-charge ratio, appearance energy, isotopic abundance and shutterability. The partial pressure p_i of the species i was determined in the usual manner,[46] based on the relation.

$$p_i = \varkappa(I_i T/\sigma_i\beta_i\gamma_i), \tag{4}$$

where $\varkappa$ is the proportionality constant, I_i the ion intensity, σ_i the relative ionization cross section, β_i the isotopic abundance, and γ_i the multiplier gain of the detector. The proportionality constant $\varkappa$ was obtained from comparison of the observed I_{Li}-to-I_{Li2} ratio with the equilibrium constant reported for the $Li_2(g)=2Li(g)$ reaction.[47] The molecular ionization cross section was calculated by taking the sum of Mann's cross sections.[48] The multiplier gain of the detector was obtained from a calibration curve.

Figure 5 shows a mass spectrum of gaseous species in molecular beams effusing from the Knudsen cell heated to 1052 K.[9] Different regions of the spectrum are shown at different intensity scales. The gaseous species were ionized by electron impact at 13.0 eV, an energy low enough to prevent the fragmentation of parent species. The bold line represents mass signals for species observed when the beam shutter was open. The thin line is the background spectrum observed while the shutter was closed. The mass peaks at m/z 52, 53, and 54 in the mass spectrum indicated the presence of the CLi_6 molecule with the natural isotopic abundance. No distinct signals were observed for another interesting molecule CLi_5 (m/z, 45—47).

Substituting the observed signal intensities for I_i in Eq. 4, one can obtain the equilibrium partial pressures of molecules in the cell. Figure 6 illustrates the partial pressures of Li(g), $Li_2(g)$, $CLi_3(g)$, $CLi_4(g)$, and $CLi_6(g)$ as a function of the reciprocal temperature. From the equilibrium constant K_p evaluated from the partial pressures measured in the range 961—1161 K and the thermodynamic relation

$$-\Delta H^\circ_{298}/T = R\ln K_p + \Delta[(G^\circ_T - H^\circ_{298})/T], \tag{5}$$

the enthalpy of Reaction (3) was determined as $\Delta H^\circ_0 = 274\pm11$ kJ mol^{-1}. This value agreed well with the theoretical value, $\Delta H^\circ_0 = 273$ kJ mol^{-1}, reported by Schleyer et al.[14] Agreement of the experimental value with the theoretical value and the mass spectrometric evidence for the species provides proof for the existence of the hyperlithiated molecule CLi_6.

Thermochemical Properties of Li_nA (A=C, O, P, S)

With Knudsen effusion mass spectrometry, Kudo et al.[7,8,12] have extended the search for other hyperlithiated molecules and determination of their thermochemical properties. Dissociation energies of the hyperlithiated molecules, Li_nA (A=C, O, P, S), determined in a series of experiments are summarized in Table 1. These values are the energies necessary to break a Li–A bond to give $Li_{n-1}A$ and Li. For CLi_6, the dissociation energy to lose Li_2 is listed. It is seen that all of the hyperlithiated molecules listed here are stable toward loss of a lithium atom. Namely, it was confirmed that the hyperlithiated molecules with nine or more valence electrons were thermodynamically more stable than the corresponding octet molecules with eight valence electrons.

Another value to be taken into account is the contributing bond energy (CBE), which is equivalent to an average bond energy in molecules. In Fig. 7, the CBEs of Li_nA are plotted as a function of the number of lithium atoms. Although the dissociation energy tends to decrease with increasing number of the constituent lithium atoms, the average C–Li bond energy (252 ± 11 kJ mol^{-1}) of CLi_6 with $n=6$ is higher than the Cl–Cl bond energy (243.5 kJ mol^{-1})[49] in Cl_2, an octet molecule. The average bond energies in Li_4P (Li–P, 218 ± 35 kJ mol^{-1}) and Li_4S (Li–S, 225 ± 38 kJ mol^{-1}) are still high compared with the bond energy for F–F (157.7 kJ mol^{-1}), Br–Br (192.9 kJ mol^{-1}), and I–I (150.6 kJ mol^{-1}) molecules.[49]

The ionization energy is also an important thermochemical value for understanding the nature of bonding. Table 2 lists the theoretical and experimental values of ionization energies (IP) for hypervalent molecules detected in our experiments.[11,17,24,25,44,45] The experimental values were measured by electron impact ionization using a mass spectrometer. Theoretical values are the vertical ionization energy, calculated as the multireference single- and double-

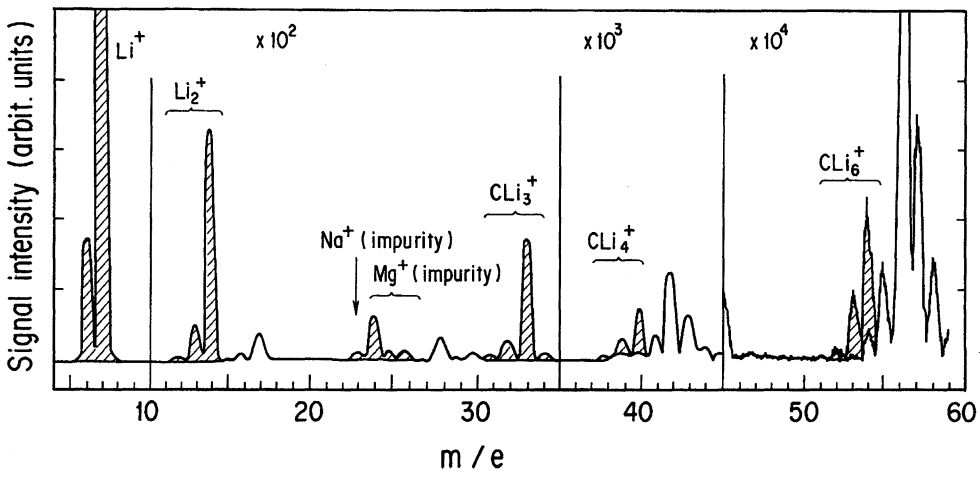

Fig. 5. Mass spectrum of gaseous species in molecular beams effusing from Knudsen cell containing $Li_2C_2(s)$ at 1025 K. The gaseous species were ionized by electron impact at 13.0 eV.

excitation configuration interaction (MRCI) energy of Li_nA^+ ions relative to that of the neutral Li_nA species at the energy minimum. The experimental values agree reasonably well with the theoretical values.

Structures and Bonding of Li_3S and Li_4S

In comparison with Li_3O and Li_4O molecules, it is interesting to elucidate the nature of bonding in Li_3S and Li_4S. Although the experimental procedure provides sufficiently accurate thermochemical data, we need information about molecular structures to understand the nature of bonding in hyperlithiated molecules. No experimental spectroscopic data are available at present, but theoretical calculations reveal features of structures and bonding in great detail for all

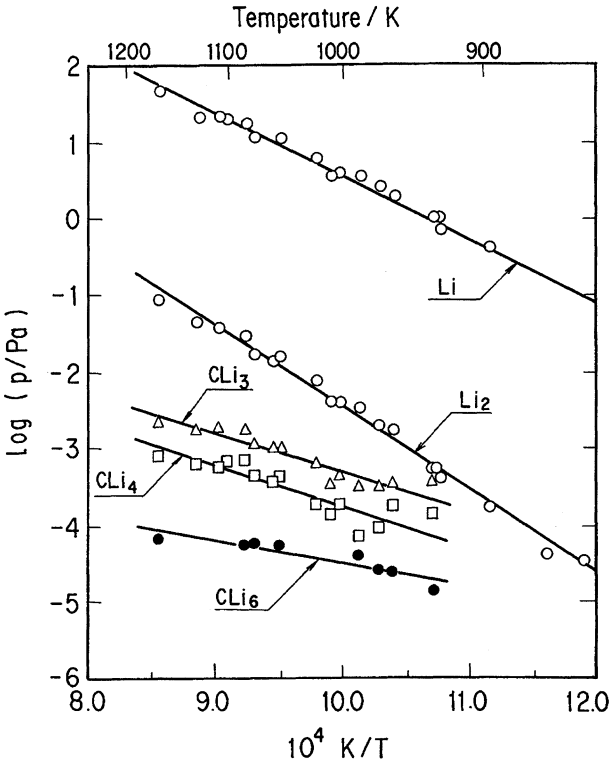

Fig. 6. Equilibrium partial pressures of gaseous species over $Li_2C_2(s)$ as a function of the reciprocal temperature.

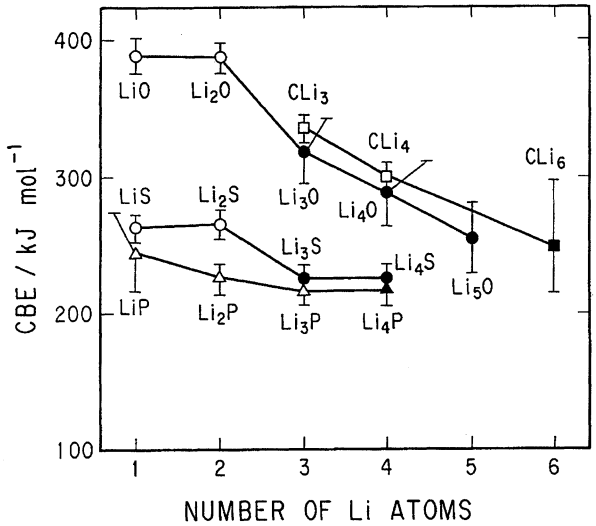

Fig. 7. Average Li–A bond energies (CBE) in Li_nA species. The closed marks represent hypervalent molecules.

Table 2. First Ionization Energies of Hypervalent Molecules

Process	IP/eV		
	Theoretical[a]		Experimental
	Schleyer et al.[24,25]	Kudo et al.	Kudo et al.
$CLi_6 \rightarrow CLi_6^+$	—	4.08	<9
$Li_3O \rightarrow Li_3O^+$	3.48	—	4.5±0.2
$Li_4O \rightarrow Li_4O^+$	4.71	—	<7.3
$Li_3S \rightarrow Li_3S^+$	3.61	4.11	4.4±0.2
$Li_4S \rightarrow Li_4S^+$	—	4.09	—
$Li_4P \rightarrow Li_4P^+$	3.40	—	—
$Li_2CN \rightarrow Li_2CN^+$	—	5.13	5.4±0.2
$Na_2CN \rightarrow Na_2CN^+$	—	4.66	4.9±0.2
$K_2CN \rightarrow K_2CN^+$	—	3.70	4.0±0.2

a) The vertical ionization energy.

stationary points on the potential energy surface. By using the MRCI method, ab initio MO calculations were carried out to obtain theoretical values of vertical ionization energies (IP) as well as dissociation energies of the Li_nS (n=1—4) molecules (Table 4).[12]

The molecular structures with a potential energy minimum were optimized at the MP2(FU)/6-31+G* level. The atomic natural orbital basis set[50] with contractions of [5s3p2d] for S and [4s3p2d] for Li was used in the configuration interaction (CI) calculations. The reference wave functions were generated by a complete active space self-consistent field (CASSCF) procedure. The configurations with $|c_i|>0.05$ were selected as the reference configurations in the CI calculations, and then 400000—1300000 configuration state functions (CSFs) were considered through single and double substitutions from the reference configurations. The calculated CI energies were converted to estimate full CI energies with the Davidson correction.[51] The GAUSSIAN92[52] and MOLCAS2[53] programs were used in these calculations.

The molecular parameters of Li_nS (n=1—4) molecules are listed in Table 3. With respect to Li_2S, Li_3S, and Li_4S Schleyer's group[24] has also searched for the global minima at the MP2(FU)/6-31+G* level, and reported that the most stable structures of Li_2S, Li_3S, and Li_4S have C_{2v}, C_{3v}, and C_{2v} symmetry, respectively. Marsden[20] has reported that the C_{2v} structure of Li_4S is the most stable with MP4SDQ/6-31G*//UHF/3-21G(*) and that the second most stable geometry C_{3v} is 1.7 kJ mol^{-1} higher than the C_{2v} structure. We found that the C_{2v} structure (shown in Fig. 9) is 7.9 kJ mol^{-1} more stable than the C_{3v} structure.

Table 4 lists theoretical dissociation energies (D_0°) and ionization energies (IP) of Li_nS (n=1—4) molecules calculated by the MRCI method. The ab initio MO calculations indicates that occupancy of the nine valence electrons in Li_3S is $(5a_1)^2(3e)^4(6a_1)^2(7a_1)^1$ and that 10 valence electrons in Li_4S are in the configuration of $(6a_1)^2(3b_1)^2(7a_1)^2(3b_2)^2(8a_1)^2$. Figure 8 shows an energy diagram of these molecular orbitals. The highest orbital, $7a_1$, of Li_3S is singly occupied (SOMO). The $8a_1$ orbital of Li_4S is HOMO. The SOMO of Li_3S and HOMO of Li_4S are antibonding between the lithium and sulfur atoms, but are bonding between all pairs of lithiums in these molecules. In spite of the antibonding character

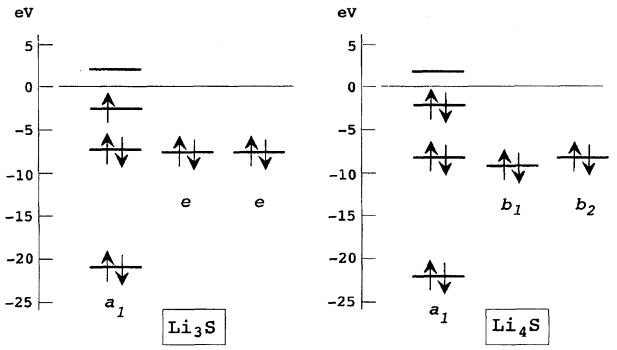

Fig. 8. Valence molecular orbital energy diagrams of Li_3S and Li_4S calculated at the HF/STO-3G level. Core orbitals are not shown here.

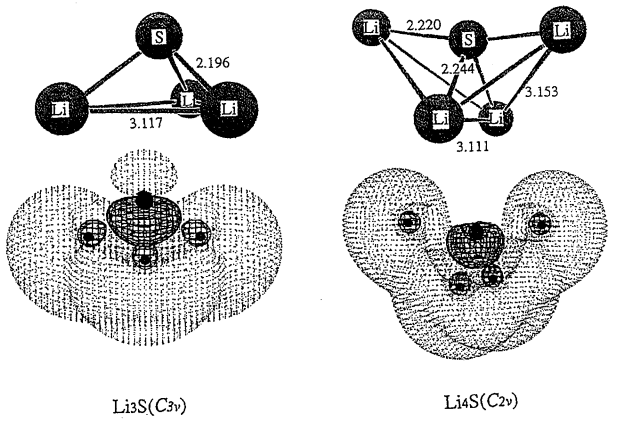

Fig. 9. Features of SOMO in Li_3S (C_{3v}) and HOMO in Li_4S (C_{2v}) deduced from theoretical calculations at UHF/STO-3G level. The SOMO and HOMO are antibonding between Li and S, but bonding between all pairs of lithiums in these molecules.

of SOMO and HOMO, the central atom is bound to lithiums through an electrostatic interaction. The charges calculated by the natural bond orbital (NBO) analysis are +0.62 (×3) on lithium and −1.88 on sulfur in Li_3S, and +0.71 (×2) and +0.25 (×2) on lithium and −1.94 on sulfur in Li_4S. The extra electrons contribute to the formation of a metallic cage with Li–Li bonding, similar to CLi_6, Li_3O, and Li_4O. Figure 9 illustrates features of the SOMO and HOMO of Li_3S (C_{3v}) and Li_4S (C_{2v}) molecules calculated at the HF/STO-

Table 3. Vibrational Frequencies and Geometries of Li_nS Molecules Calculated at the MP2(FU)/6-31+G* Level

Molecule	Point group	ZPE[a]	Frequency	Geometry
		kJ mol^{-1}	cm^{-1}	
LiS	C_∞	3.3	σ: 569	2.186 Å(Li-S)
Li_2S	C_{2v}	7.9	a_1: 583,128	2.116 Å(LiS)
			b_2: 637	104.4° (∠LiSLi)
Li_3S	C_{3v}	11.7	a_1: 546,144	See Fig. 9
			e: 507,119	
Li_4S	C_{2v}	15.5	a_1: 491, 438, 158, 119	See Fig. 9
			b_1: 449, 143	
			b_2: 506, 131	

a) Zero-point vibrational energy.

Table 4. Theoretical Ionization Energies (IP) and Dissociation Energies ($D_0°$) of Li_nS (n=1—4) Molecules Calculated by the MRCI Method

	Total energy[a]	n[b]	CSF[c]	$\sum c_i^2$	IP[d]	D_0°
	E_h				eV	kJ mol^{-1}
$LiS(^2\Pi)$	−405.167729	9	69748	0.937		
$LiS^+(^3\Sigma^-)$	−404.887594	5	25937	0.944	7.62	
$LiS^+(^1\Delta)$	−404.838953	8	31643	0.949	8.95	
Li+S	−405.058227	6	52774	0.947		284.1
$Li_2S(^1A_1)$	−412.709198	6	101671	0.915		
$Li_2S^+(^2B_1)$	−412.477444	7	138124	0.938	6.30	
$Li_2S^+(^2A_1)$	−412.462995	7	116637	0.937	6.70	
LiS+Li	−412.275199	6	209230	0.932		281.2
$Li_3S(^2A_1)$	−420.198147	5	368079	0.908		
$Li_3S^+(X^1A_1)$	−420.047223	9	465807	0.928	4.11	
$Li_3S^+(\mathbf{1}^3A_1)$	−419.916502	2	179435	0.920	7.66	
$Li_3S^+(\mathbf{1}^1A_2)$	−419.905086	4	428579	0.921	7.97	
$Li_3S^+(\mathbf{2}^1A_1)$	−419.901900	13	613658	0.915	8.06	
Li_2S+Li	−420.141567	5	481721	0.921		148.5
$Li_4S(^1A_1)$	−427.672234	4	137011	0.902		
$Li_4S^+(^2A_1)$	−427.672230	4	186240	0.911	4.09	
Li_3S+Li	−427.631082	4	1077606	0.908		102.5

a) Estimated full CI energy with Davidson's correction. b) Number of reference configurations. c) Number of configuration state functions. d) The vertical ionization energy.

3G level. The SOMO of Li_3S seems to build the cage. The widely spreading HOMO of Li_4S suggests more clearly the lithium cage formation in the molecule.[12]

We can summarize the bonding situation in Li_nA (A=C, O, P, S) molecules as follows: the octet of valence electrons in Li_nA molecules is involved in A–Li bonding. The extra valence electrons in the hyperlithiated molecules are not associated with the central atom, but contribute to the formation of metallic lithium cage. The overall features can be described in terms of a negatively charged center (A^{m-}) embedded in a positively charged lithium cage or cluster (Li_n^{m+}). Analogous explanations are possible for bonding in the hyperaluminum molecules, Al_3O and Al_4O,[35] and the hypermagnesium molecules, Mg_2O, Mg_3O, and Mg_4O,[37] which have the electronegative oxygen atom in the interior of the electropositive cluster. In the hypersilicon molecules like Si_2O and Si_3O, however, the bonding situation is different from hypervalent molecules described above, although the silicon–oxygen attraction is largely ionic. Theoretical calculations by Boldyrev and Simons[39] have indicated that an oxygen atom favors coordination to the periphery of silicon clusters rather than insertion into Si–Si bonds. Structures with the oxygen inside the cluster are much higher in energy. This is in contrast with the structures of other oxygen–metal clusters, such as Li_3O, Li_4O, Mg_2O, Mg_3O, Mg_4O, Al_2O, Al_3O, and Al_4O, where the oxygen atom inserts into the site of highest coordination and highest symmetry. Anyway, the substantial stability of these hypervalent molecules is due to the high degree of ionic character as well as bonding interactions between the metal atoms.

Another Type of Hypervalent Molecules M_2CN (M=Li, Na, K)

Recently, Kudo's group has detected another type of hyperlithiated molecule Li_2CN in the equilibrium vapor over a mixture of lithium metal and NaCN by means of Knudsen-effusion mass spectrometry.[17] The experimental dissociation energy to give LiNC and Li, D_0°(LiNC–Li)=137±14 kJ mol^{-1}, agreed reasonably with the theoretical value (104 kJ mol^{-1}) calculated by the MRCI method. The first ionization energies, 9.24±0.2 and 5.39±0.2 eV, determined for both the LiNC and Li_2CN molecules agreed well with the theoretical values for vertical ionization as listed in Table 2. The agreement between experiment and theory confirms the existence of the Li_2CN species, which is possibly the first hyperlithiated species with more than one electronegative atom. Actually, theoretical calculations have indicated that the favored structure has C_s symmetry and the species would consist of the Li_2^+ radical cation and the CN^- anion, the bonding feature being apparently different from those of Li_nA (A=C, O, P, S) species described in the previous section. The presence of a Li_2^+ unit justifies the term hyperlithiated for this system.

Computational geometry optimization at MP2(FU)/6-31G* and MP2(FC)/6-31+G* gives four possible isometric structures to the Li_2CN molecule; i.e. the planar structures **7** and **8** with C_s symmetry and the linear structures **9** and **10** with $C_{\infty v}$ symmetry (Fig. 10). The latter two isomers are "electronomers".[54,55] All of the isomers have a short C–N bond length (ca. 1.19 Å), indicative of a triple bond between C and N. The calculated Wiberg bond index also indicates triple-bond or near-triple-bond character for **7**—**10**. The global minimum is **7**, although **8** is only 0.8 kJ mol^{-1} less

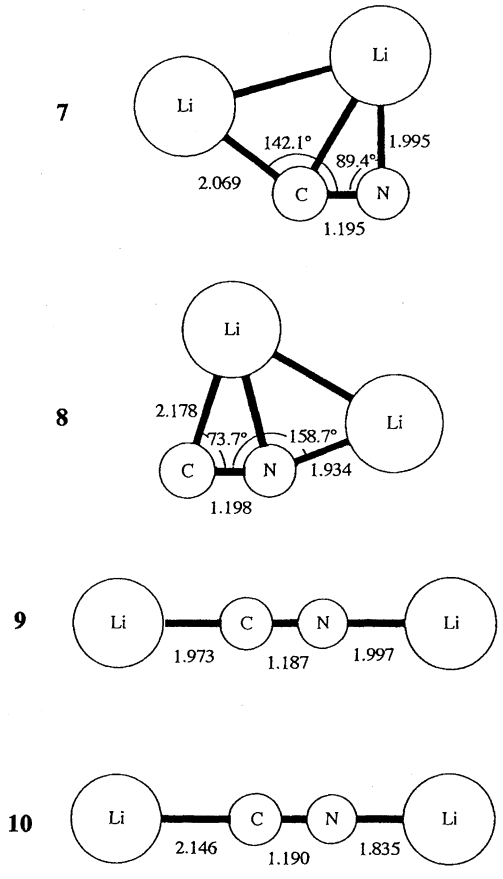

Fig. 10. Optimized structures of Li_2CN; the bond distance in Å. In these isomers, **7** is the most stable and **8** is only 0.8 kJ mol^{-1} less stable than **7**. Structures **9** and **10** are 40 and 37 kJ mol^{-1} higher in energy than **7**, respectively, at QCISD(T)(FC)/6-31+G*//MP2(FU)/6-31G*.

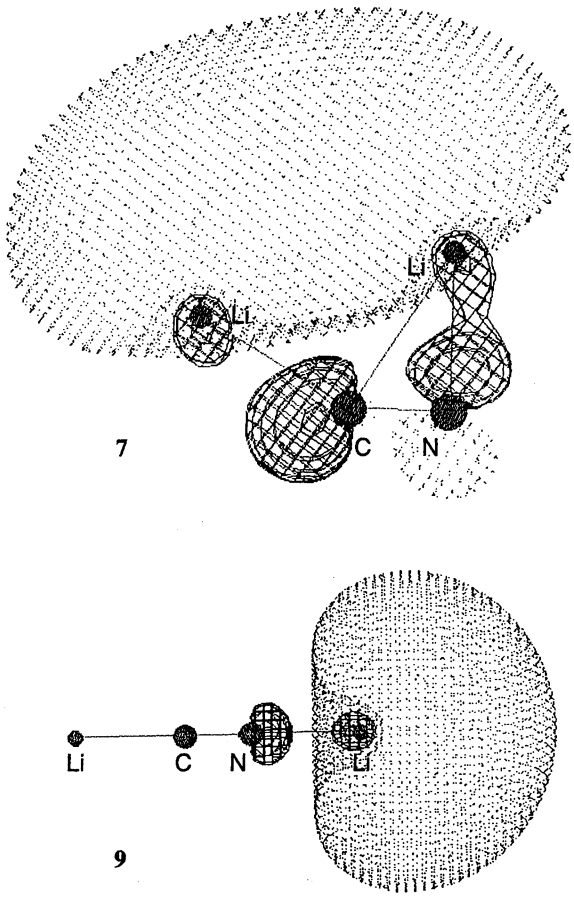

Fig. 11. Features of SOMO in Li_2CN species deduced from MP2(FC)/6-31G* calculations; **7** the planar [$Li_2^+(CN)^-$] and **9** the linear [$Li^+(CN)^-Li\cdot$].

stable at QCISD(T)(FC)/6-31+G*//MP2(FU)/6-31G*. At this level, structures **9** and **10** are 40 and 37 kJ mol^{-1} higher in energy than **7**, respectively. MRCI calculations give a similar picture; **7** and **8** have almost the same energy, with **8** being favored by 0.04 kJ mol^{-1} and with **9** and **10** being 36 and 50 kJ mol^{-1} less stable than **7**, respectively. Density functional calculations (BLYP/6-31G(2df)) also favor **7** (0.8 kJ mol^{-1}) over **8**, with both **9** and **10** being about 40 kJ mol^{-1} higher in energy than **7**. Thus, only the planar isomers **7** and **8** with C_s symmetry are stable structures.

The valence molecular orbitals of Li_2CN (**7**,**8**) with C_s symmetry are described as $(5a')^2(6a')^2(7a')^2(1a'')^2(8a')^2(9a')^1$. The 9a′ singly occupied orbital (SOMO) corresponds to the Li_2^+ radical cation MO and contributes to Li–Li bonding, as shown in Fig. 11. The other electrons are distributed around the CN moiety. The in-plane valence electron density of **7** and **8** reveals the interaction between the Li_2^+ and CN^- units, and the planar Li_2CN molecules can both be described as complexes of a cyanide anion with a Li_2^+ radical cation. This description is confirmed both by the short Li–Li distance of about 2.6 Å, which is very similar to that calculated for Li_2^+ (2.63 Å at MP2/6-31G*), and by the natural charges of about +0.5 on each lithium center in **7** and **8**. Thus, Li_2CN is another example of a species in which a charged Li_n^{m+} fragment (here Li_2^+) is present. The existence of such transferable charged fragments in perlithiated and hyperlithiated species has recently been pointed out by Schleyer's analysis of C_2Li_6 and C_2Li_4[56] and extensions of Marsden's work on CLi_8 and CLi_{12}.[21]

The valence molecular orbitals of Li_2CN (**9**,**10**) with $C_{\infty v}$ symmetry are described as $(3\sigma)^2(4\sigma)^2(2\pi)^2(5\sigma)^2(6\sigma)^1$ and the extra electron is localized on either of the Li atoms. The linear LiCNLi structure **9** is a minimum, but **9** is 40 kJ mol^{-1} higher in energy than **7**. The extra valence electron in SOMO of **9** is localized on the Li atom near the N atom, as shown in Fig. 11. On the other hand, the extra valence electron of **10** is localized on the Li atom near C atom. Hence, these "electronomers"[54,55] can be described as $Li^+(CN)^-Li\cdot$(**9**) and $Li\cdot(CN)^-Li^+$ (**10**). The similar energies of **9** and **10** reflect the comparable stabilities of LiCN and LiNC.

In addition to Li_2CN, the existence of hypervalent Na_2CN and K_2CN molecules has also been demonstrated by mass spectrometric observations as well as ab initio MO calculations.[33,34] The dissociation energies and ionization energies of M_2CN (M=Li, Na, K) molecules are summarized in Table 1. The experimentally determined dissociation energy of Na_2CN to give NaCN and Na, D_0°(NaCN–Na)=104±13

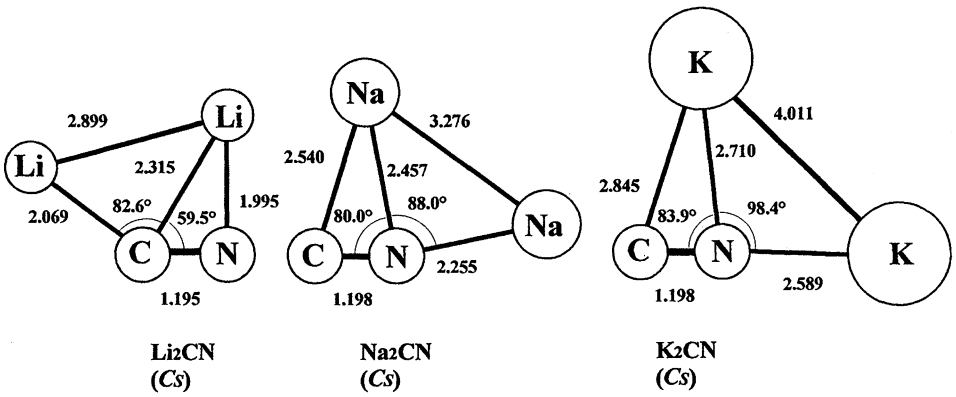

Fig. 12. The most stable structures of Li_2CN, Na_2CN, and K_2CN obtained at MP2(FU)/6-31G*; the bond length in Å.

kJ mol^{-1}, was smaller than that of Li_2CN to give LiNC and Li, D_0°(LiNC–Li)=137±14 kJ mol^{-1}. The dissociation energy, D_0°(KCN–K)=85±15 kJ mol^{-1}, determined for K_2CN to give KCN and K was the smallest of these species. It should be noticed here that the dissociation products of Na_2CN and K_2CN are different from that of Li_2CN. The former two molecules give cyanides while the latter gives isocyanide.[55—60]

Both Na_2CN and K_2CN are theoretically revealed to have isomeric structures similar to Li_2CN (two planar structures with C_s symmetry and two linear electronomers with $C_{\infty v}$ symmetry), although there are differences in the bond lengths and bond angles. The theoretically predicted structures of planar Na_2CN and K_2CN — the most stable at the MP2(FC)/6-31G* level — are depicted in Fig. 12, in comparison with that of Li_2CN **7**. The valence molecular orbitals of planar Na_2CN and K_2CN are described as $(11a')^2(12a')^2(13a')^2(2a'')^2(14a')^2(15a')^1$ and $(17a')^2(18a')^2(19a')^2(3a'')^2(20a')^2(21a')^1$, respectively. The SOMOs of 15a′ and 21a′ correspond to the radical-cation orbitals of Na_2^+ and K_2^+, respectively, and contribute to Na–Na and K–K bonding. The other electrons are distributed around the CN moiety. Thus, the bonding situations among these hypervalent species M_2CN (M=Li, Na, K) are considered essentially the same.

Conclusion

Following the experimental discovery of a hyperlithiated molecule Li_3O, ab initio MO calculations predicted that replacement of hydrogen atoms by lithium atoms in hydrides of second- and third-row elements in the periodic table would give hyperlithiated molecules with stoichiometries exceeding normal valence expectation. A number of experimental and theoretical investigations have provided evidence that hyperlithiated molecules are thermodynamically stable, despite of their unusual stoichiometries. Until now, the existence of such hyperlithiated molecules as CLi_6, Li_4O, Li_5O, Li_3S, Li_4S, and Li_4P has been confirmed. These molecules have 9 or 10 valence electrons, violating, at least formally, the octet rule. The results of ab initio MO calculations have revealed that the extra electrons in Li_nA (A=C, O, P, S) molecules are not associated with the cental atom, which remains content with its normal octet. Instead the extra electrons beyond the usual octet are in SOMO or HOMO, totally symmetric orbitals, and the Li–Li bonds between all pairs of lithium atoms contribute to the formation of a metallic cage. The overall bonding in Li_nA molecules can be described in terms of the electrostatic attraction between the electronegative central atom (A^{m-}) and the electropositive surrounding cage or cluster (Li_n^{m+}).

Furthermore, experimental evidence has been obtained for another type of hyperlithiated or hypervalent species, the bonding situation of which is apparently different from those described above. These species are Li_2CN, Na_2CN, and K_2CN with more than one electronegative atom. Of these species, Li_2CN is the most stable toward dissociation; i.e. the dissociation energies determined are D_0°(LiNC–Li)= 137±14 kJ mol^{-1}, D_0°(NaCN–Na)=104±13 kJ mol^{-1}, and D_0°(KCN–K)=85±15 kJ mol^{-1}. Theoretical calculations indicate that these species would be composed of the M_2^+ (M=Li, Na, K) radical cation and the CN^- anion. The short C–N bond length (ca. 1.19 Å) is indicative of a triple bond between C and N. The presence of the M_2^+ unit justifies the term hypervalent for these systems. The extra valence electron in SOMO corresponds to the M_2^+ radical cation, and contributes to M–M bonding. In addition, these molecules are revealed to have four stable isomers slightly different in energy; the planar structures are more stable than the linear structures. The linear structures of M_2CN are electronomers and best described as complexes like $M^+(CN)^-M\cdot$ and $M\cdot(CN)^-M^+$.

References

1) G. N. Lewis, *J. Am. Chem. Soc.*, **38**, 762 (1916).
2) W. Kossel, *Ann. Phys.*, **49**, 229 (1916).
3) H. Kudo, C. H. Wu, and H. R. Ihle, *J. Nucl. Mater.*, **78**, 380 (1978).
4) C. H. Wu, H. Kudo, and H. R. Ihle, *J. Chem. Phys.*, **70**, 1815 (1979).
5) H. Kudo, *Chem. Lett.*, **1989**, 1611.
6) C. H. Wu, *Chem. Phys. Lett.*, **139**, 357 (1987).
7) H. Kudo and C. H. Wu, *Chem. Express*, **5**, 633 (1990).
8) H. Kudo and K. F. Zmbov, *Chem. Phys. Lett.*, **187**, 77 (1991).
9) H. Kudo, *Nature*, **355**, 432 (1992).

10) H. Kudo and C. H. Wu, *J. Nucl. Mater.*, **201**, 261 (1993).
11) H. Kudo, *J. Mass Spectrom. Soc. Jpn.*, **41**, 317 (1993).
12) H. Kudo, K. Yokoyama, and C. H. Wu, *J. Chem. Phys.*, **101**, 4190 (1994).
13) P. v. R. Schleyer, E.-U. Würthwein, and J. A. Pople, *J. Am. Chem. Soc.*, **104**, 5839 (1982).
14) P. v. R. Schleyer, E.-U. Würthwein, E. Kaufmann, T. Clark, and J. A. Pople, *J. Am. Chem. Soc.*, **105**, 5930 (1983).
15) P. v. R. Schleyer, "New Horizons of Quantum Chemistry," ed by P.-O. Löwdin and B. Pullman, Reidel Publ., Dortrecht (1986), p. 95.
16) W. J. Hehre, L. Radom, P. v. R. Schleyer, and J. A. Pople, "*Ab initio* Molecular Orbital Theory," John Wiley & Sons, New York (1986), p. 425.
17) H. Kudo, M. Hashimoto, K. Yokoyama, C. H. Wu, A. E. Dorigo, F. M. Bickelhaupt, and P. v. R. Schleyer, *J. Phys. Chem.*, **99**, 6477 (1995).
18) A. E. Reed and F. Weinhold, *J. Am. Chem. Soc.*, **107**, 1919 (1985).
19) J. P. Ritchie and S. M. Bacharach, *J. Am. Chem. Soc.*, **109**, 5909 (1987).
20) C. J. Marsden, *J. Chem. Soc., Chem. Commun.*, **1989**, 1356.
21) J. Ivanic and C. J. Marsden, *J. Am. Chem. Soc.*, **115**, 7503 (1993).
22) J. Ivanic, C. J. Marsden, and D. M. Hassett, *J. Chem. Soc., Chem Commun.*, **1993**, 822.
23) G. L. Gutsev and A. I. Boldyrev, *Chem. Phys. Lett.*, **92**, 262 (1982).
24) a) E. Rehm, A. I. Boldyrev, and P. v. R. Schleyer, *Inorg. Chem.*, **31**, 4834 (1992) ;b) P. v. R. Schleyer, private communication (1993).
25) V. G. Zakrewski, W. von Niessen, A. I. Boldyrev, and P. v. R. Schleyer, *Chem. Phys. Lett.*, **197**, 195 (1992).
26) M. Gutovski and J. Simons, *J. Phys. Chem.*, **98**, 8326 (1994).
27) Z. Shi, J. Wang, and R. J. Boyd, *J. Phys. Chem.*, **99**, 4941 (1995).
28) K. I. Peterson, P. D. Dao, and A. W. Castlemann, Jr., *J. Chem. Phys.*, **79**, 1977 (1984).
29) P. D. Dao, K. I. Peterson, and A. W. Castlemann, Jr., *J. Chem. Phys.*, **80**, 563 (1984).
30) E.-U. Würthwein, P. v. R. Schleyer, and J. A. Pople, *J. Am. Chem. Soc.*, **106**, 6973 (1984).
31) S. Pollack, C. R. Chris Wang, and M. M. Kappes, *Chem. Phys. Lett.*, **175**, 209 (1990).
32) Z.-L. Cai, G. Hirsch, and R. J. Buenker, *Chem. Phys. Lett.*, **246**, 529 (1995).
33) C. Ochsenfeld, J. Gauss, and R. Ahlrichs, *J. Chem. Phys.*, **103**, 7401 (1995).
34) C. Ochsenfeld, J. Gauss, and R. Ahlrichs, *J. Chem. Phys.*, **101**, 5977 (1994).
35) A. I. Boldyrev and P. v. R. Schleyer, *J. Am. Chem. Soc.*, **113**, 9045 (1991).
36) V. G. Zakrewski, W. von Niessen, A. I. Boldyrev, and P. v. R. Schleyer, *Chem. Phys.*, **174**, 167 (1993).
37) A. I. Boldyrev, I. L. Shamovsky, and P. v. R. Schleyer, *J. Am. Chem. Soc.*, **114**, 6469 (1992).
38) A. I. Boldyrev, J. Simons, and P. v. R. Schleyer, *Chem. Phys. Lett.*, **233**, 266 (1995).
39) A. I. Boldyrev and J. Simon, *J. Phys. Chem.*, **97**, 5875 (1993).
40) J. Moc and K. Morokuma, *J. Am. Chem. Soc.*, **117**, 11790 (1995).
41) C. J. Marsden, *Chem. Phys. Lett.*, **245**, 475 (1995).
42) E. D. Jemmis, J. Chandrasekhar, E.-U. Würthwein, P. v. R. Schleyer, J. W. Chin, Jr., F. J. Landro, R. J. Lagow, B. Luke, and J. A. Pople, *J. Am. Chem. Soc.*, **104**, 4275 (1982).
43) J. W. Chinn, Jr., and R. J. Lagow, *J. Am. Chem. Soc.*, **106**, 3694 (1984).
44) M. Hashimoto, K. Yokoyama, H. Kudo, C. H. Wu, and P. v. R. Schleyer, *J. Phys. Chem.*, to be published.
45) M. Hashimoto, K. Yokoyama, H. Kudo, C. H. Wu, and P. v. R. Schleyer, *J. Phys. Chem.*, to be published.
46) R. T. Grimley, "The Characterization of High Temperature Vapors," ed by J. L. Magrave, Wiley, New York (1967), p. 195.
47) C. H. Wu, *J. Chem. Phys.*, **65**, 3181 (1976).
48) J. B. Mann, *J. Chem. Phys.*, **46**, 1646 (1967).
49) A. G. Massay, "Main Group Chemistry," Ellis Horwood, Chinchester (1990), p. 340.
50) H. F. Schaefer, III, "Method of Electronic Structure Theory," ed by B. O. Roos and P. E. M. Siegbahn, Plenum, New York (1977), p. 277.
51) P.-O. Widmark, P. Å. Malmqvist, and B. O. Roos, *Theor. Chim. Acta*, **77**, 291 (1990).
52) M. J. Frisch, G. W. Trucks, M. Head-Gordon, P. M. W. Gill, M. W. Wong, J. B. Foresman, B. G. Johnson, H. B. Achlegel, M. A. Robb, E. S. Replogle, R. Gomperts, J. L. Abdres, K. Raghavachari, J. S. Binkley, C. Gonzalez, R. L. Martin, D. J. Fox, D. J. Defrees, J. Baker, J. J. P. Stewart, and J. A. Pople, "GAUSSIAN92, Revision C.4," Gaussian, Pittsburgh, PA (1992).
53) K. Andersson, M. R. A. Blomberg, M. P. Fülscher, Y. Kellö, R. Lindh, P.-Å. Malmqvist, J. Noga, J. Olsen, B. O. Roos, A. J. Sadlej, P. E. M. Siegbahn, M. Urvan, and P.-O. Widmark, "MOLCAS, Version 2," University of Lund, Lund, Sweden (1992).
54) A. Dorigo and P. v. R. Schleyer, *Chem. Phys. Lett.*, **186**, 363 (1991).
55) A. Dorigo, P. v. R. Schleyer, and P. Hobza, *J. Comput. Chem.*, **15**, 322 (1994).
56) A. E. Dorigo, N. J. R. v. E. Hommes, K. Krogh-Jespersen, and P. v. R. Schleyer, *Angew. Chem., Int. Ed. Engl.*, **31**, 1602 (1992).
57) B. Bak, E. Clementi, and E. K. Kortsenborn, *J. Chem. Phys.*, **52**, 764 (1970).
58) C. J. Marsden, *J. Chem. Phys.*, **76** 6451 (1982).
59) J. J. van Vaals, W. L. Meerts, and A. Dynamus, *Chem. Phys.*, **82**, 385 (1983).
60) L. Admovicz and C. I. Frum, *Chem. Phys. Lett.*, **157**, 496 (1989).

Hiroshi Kudo was born in Qingdao, China in 1941. He received both his B.S. (1964) and M.S. (1967) degrees from Tohoku University. He joined the Japan Atomic Energy Research Institute (JAERI) as a research scientist in 1967. He received his D.Sc. from Tohoku University in 1971 on radiochemistry of nuclear recoil. From 1976 to 1977, he stayed in Kernforschungsanlage Jülich, Germany as a research fellow from the Science and Technology Agency. In Jülich he detected the hyperlithiated molecule Li_3O for the first time. He was promoted Principal Scientist (1984) and to Head of Division for Isotope Research and Development, JAERI (1988), where he worked on tritium chemistry for nuclear fusion. Since 1993, he has extended his studies on hyperlithiated molecules in Advanced Science Research Center, JAERI, in collaboration with Professor C. H. Wu of Max-Planck-Institut and Professor P. v. R. Schleyer of Erlangen Universität. He was appointed as Professor, Department of Chemistry, Faculty of Science, Tohoku University in 1994. He received Divisional Award of the Chemical Society of Japan in 1996.

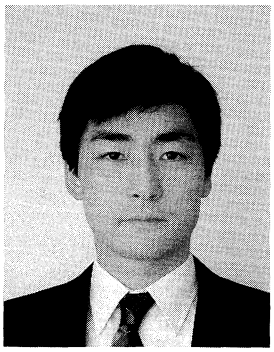

Keiichi Yokoyama was born in Osaka in 1962. He was graduated (1986) and received his Ph.D. degree (1991) from Osaka University on the reaction dynamism of the nitrogen-containing reaction intermediates under the supervision of Professor T. Fueno. He joined the Japan Atomic Energy Research Institute as a research scientist in 1991. His current research concerns reaction dynamics of small molecules and molecular structures and stability of hyperlithiated molecules by means of laser- and molecular-beams experiments and computations.